Field-driven reorientation in ultrathin ferromagnetic films with uniaxial anisotropy

H. P. Oepen, Y. T. Millev,* H. F. Ding, S. Pütter, and J. Kirschner
Max-Planck-Insitut für Mikrostrukturphysik, Weinberg 2, 06120 Halle, Germany
(Received 26 July 1999; revised manuscript received 19 November 1999)

The field-driven spin reorientation transition in uniaxial in-plane magnetized films is discussed by means of phase diagrams which are obtained from the stability analysis of the thermodynamical potential. A classification of the field induced reorientation is carried out concerning the anisotropy axes in films grown on vicinal and twofold low-index surfaces. It is shown that hard-axis loops with magnetization flop are directly related to the reorientation in field. In the framework of the general theory the hard-axis loops can be precisely analyzed.

I. INTRODUCTION

Many ferromagnetic films grown on vicinal low-index surfaces exhibit uniaxial in-plane anisotropy.[1–4] Vicinal surfaces are unique in so far as they provide the flexibility to tune the strength of the anisotropy by changing the miscut angle, i.e., the step density.[5,6] The uniaxial anisotropy of such films is also used to study the effect of morphology and deposition of nonmagnetic metals on the magnetic properties.[7,8] Magneto-optical Kerr effect (MOKE) experiments are performed in these studies. MOKE, however, does not directly give access to the anisotropy constants. From hard-axis measurements anisotropies are deduced under very simplified assumptions.[8]

Recently, the influence of external fields on the magnetization in uniaxial systems has been investigated.[9] In a second-order anisotropy approximation it was demonstrated that the spin reorientation can follow different scenarios under an applied field, depending on the ratio of the first- and second-order anisotropies involved. In this paper we want to demonstrate the one-to-one correspondence of the general theory and the magnetic behavior of films with in-plane uniaxial anisotropy. We will examine the different assumptions made in different papers and demonstrate that most of them are far too crude. A detailed analysis scheme is put forward.

The paper is organized as follows. First, we will briefly summarize the main features of the hysteresis obtained in the hard axis and the notation commonly used in related papers. Section II deals with the main results of the general theory including the most relevant phase diagram in the context of this paper. Section III presents a general classification of spin reorientation in ultrathin ferromagnets grown on vicinal or low-index twofold surfaces. It will be shown that the commonly used notations of the angle-dependent free energy can directly be transformed into the mathematical structure used in the general theory. Furthermore, it will be demonstrated that the phase diagram allows one to set margins for the involved anisotropies which have to be fulfilled to find certain hard-axis magnetization loops. Finally, in the last chapter a complete analysis of hard-axis loops will be given.

The particular problem posed and solved in this paper concerns hard-axis hysteresis loops such as that shown in Fig. 1 for an ultrathin ferromagnet with in-plane uniaxial anisotropy. The magnetization curve was obtained with the magnetic field perpendicular to the step edges for Co/Cu(1117) within the film plane.[10] The plot can be taken as representative for a whole class of magnetization loops that appear in hard-axis experiments such as those in Refs. 5–8. The most obvious feature is the appearance of hysteresis centered around fields that deviate strongly from zero. The fields are commonly called switching fields H_S.[7]

On applying small fields the magnetization starts to tilt away from the easy axis until the field reaches a value slightly above H_S where a discontinuous change of magnetization occurs. Above this field the magnetization is aligned with the field direction, i.e., with the hard axis. Decreasing the field causes the magnetization to remain field-aligned even at lower fields than H_S. Strictly speaking, a field range exists in which two states of magnetization appear to be stable. We estimate the lower/upper field of discontinuous changes to appear at 57 and 61 Oe, respectively, for the data plotted in Fig. 1. The slope at zero field $s=\Delta M/\Delta H$ can be used to extrapolate the anisotropy field $H_K=M/s$ that is the field at which the system will saturate if a perfect hard-axis behavior occurs. For films grown on vicinal low-index surfaces, uniaxial as well as biaxial contributions are commonly considered in the rotational free-energy ansatz.[11,12] For systems where uniaxial and biaxial frames of reference coincide (see the following sections), the anisotropy field can be written as the sum of the uniaxial and biaxial contributions[10]

$$H_K=H_U+H_4. \tag{1}$$

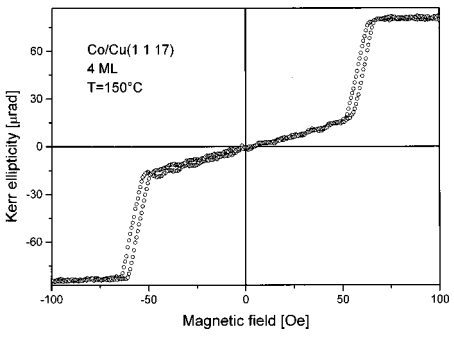

FIG. 1. Hard-axis in-plane hysteresis loop for a Co/Cu(1 1 17) film with thickness of four monolayers (ML) at 150 °C. Two discontinuous magnetization changes appear at 57 and 61 Oe.

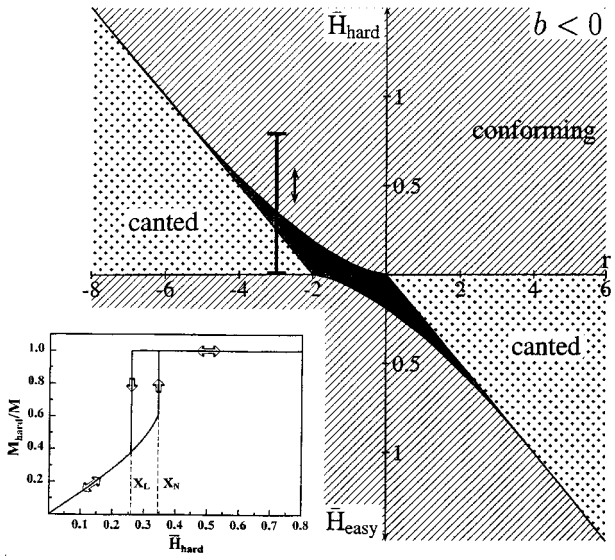

FIG. 2. Phase diagram for $b<0$ for an uniaxial ferromagnet (notation see text) in external fields. The abscissa gives the ratio r between first and second order anisotropy constant $r=a/b$. The ordinates are fields normalized with respect to the second-order anisotropy constant (see text). For the convention used in Eq. (2) the easy axis in-zero field is represented by negative r values. A field applied in the hard or easy axis is represented by the positive or negative ordinate, respectively. Cycling a field along the hard axis means to run along a vertical line in the third quadrant. Varying the field along the plotted line will give a magnetization curve as shown in the inset (for more details see text).

This expression is exactly true in the small-angle approximation. In the case of Fig. 1 we can estimate H_K to be about 300 Oe.

II. THE GENERALIZED REPRESENTATION

For a ferromagnet with uniaxial anisotropy under the influence of an external field the angle- and field-dependent contributions to the free energy can be given in a second-order approximation as

$$g(\theta)=a\sin^2\theta+b\sin^4\theta-\mathbf{H}\cdot\mathbf{M}, \tag{2}$$

where a and b represent the first- and second-order anisotropy constants, H is the external field, M the magnetization, and θ is the angle measured with respect to the easy axis of magnetization. Concentrating on the two principal geometries (those with the external field parallel and perpendicular to the easy axis), a stability analysis has been performed for the free energy of the form given in Eq. (2). Several representations of the phase diagram have been discussed in Ref. 9 including the $\bar{H}/r$ representation in which the influence of the external field on the spin reorientation can be directly explored. In the $\bar{H}/r$ representation the parameters are normalized with respect to the second-order anisotropy constant $r=a/b, \bar{H}=MH/8|b|$. Two different phase diagrams emerge depending on the sign of b. The diagram in case of negative b is given in Fig. 2.

The zero-field situation[13] for $a>0$ is retrieved along the abscissa: on the left-hand side ($r<-2$) the magnetization is aligned along the easy axis while on the right-hand side ($r>0$) the magnetization is perpendicular to that direction. The two phases are separated by a range of coexisting phases ($-2<r<0$) where both orientations correspond to local minima of the free energy. With a field applied along the hard axes two phases still do exist. One of them is aligned with the field direction (labeled ''conforming'' in Fig. 2); the other one has a canted magnetization orientation. A range of coexisting phases persists in external fields (shaded in Fig. 2). The coexisting phases are the canted and the respective neighboring aligned phase. The magnetization will cant as soon as even small fields are applied along the hard axes. An increasing field will cause the canting angle to increase and forces the system into the coexistence regime (vertical line at $r=-3$ in Fig. 2). The spin reorientation into the hard axis (the high-field conforming phase) appears after the system has been driven across the range of coexistence if we assume that the system rotates coherently following the perfect delay convention.[14] Cycling the field gives a hysteresis behavior due to the two boundaries and due to the coexistence of the two adjacent phases in the shaded regime as shown in the inset of Fig. 2.[9,15–17] This general behavior can be found in any system with uniaxial anisotropy and negative b when the magnetic fields are applied along the hard axes.

III. TRANSFORMATIONS BETWEEN EQUIVALENT ANISOTROPY EXPRESSIONS

In this section the mapping of real systems onto the very general description of Sec. II will be given. In particular, the different in-plane symmetries of low-index surfaces of fcc and bcc (including tetragonally distorted) structures will be discussed and transformed into the form of Eq. (2). Uniaxial anisotropy in the plane is considered which is found in films grown on vicinal surfaces. In the following, all possible cases are sorted out by examining the two generic possibilities of (i) easy axes aligned with in-plane axes of cubic symmetry and (ii) magnetic easy axes deviating from in-plane axes of cubic symmetry.

A. Easy axes aligned with principal axes of cubic symmetry within the plane of the film

1. Easy [100] *in-plane axis*

This situation corresponds to systems such as Fe on curved W(001) (Refs. 4,6) or Fe on vicinal Ag(001).[1,2,5] Using the notation from textbooks,[18,19] one can express the angle-dependent part of the free energy as

$$f(\alpha)=K_u\cos^2\alpha_1+K_4\cos^2\alpha_1\cos^2\alpha_2 \tag{3}$$

with K_u and K_4 called *uniaxial* and *biaxial* anisotropy constants, respectively, and with $\alpha_{1,2}$ being the angles between $\mathbf{M}$ and the two in-plane principal axes [Fig. 3(a)]. The second term is what remains from the standard lowest-order cubic invariant when one of the direction cosines is zero, since $\mathbf{M}$ is within the plane. K_4 is positive which means that the [100] directions are the easy axes for the fourfold anisotropy which would be effective if $K_u=0$. Furthermore, $K_u<0$ is assumed which means that the [100] axis is the easy axis for the uniaxial anisotropy. The case $K_u>0$ ([010] easy axis) is covered by the same equation if one chooses the 90°-rotated frame of reference. A straightforward transfor-

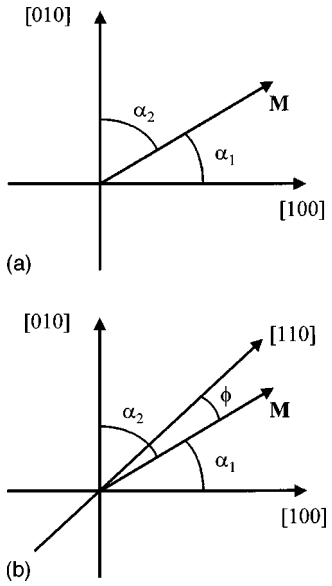

FIG. 3. Angular variables for: (a) easy axes along ⟨100⟩; (b) easy axes along ⟨110⟩ within the plane of the film.

mation brings Eq. (3) into the generalized form of Eq. (2). The identifying relations are the following:

$$a = K_4 - K_u > 0, \tag{4}$$

$$b = -K_4 < 0. \tag{5}$$

Generally, the transformations between such equivalent trigonometric expressions are linear and involve no more than a shift in the zero of the thermodynamic potential.

2. Easy [110] *in-plane axes*

Assuming the [110] axes to be the easy axes for the biaxial anisotropy contribution and, additionally, one of these as the easy axis for the uniaxial anisotropy, such as in Co/Cu(11n),[3,7] the free energy is expressed in the above notation as

$$f(\alpha) = K_u \cos^2\phi + K_4 \cos^2\alpha_1 \cos^2\alpha_2, \tag{6}$$

with $K_4 < 0$; K_u is negative as in the former case, and ϕ is the angle between **M** and the easy [110] axis [Fig. 3(b)]. Transforming again into the form of Eq. (2) yields[20]

$$a = -K_4 - K_u > 0, \tag{7}$$

$$b = K_4 < 0. \tag{8}$$

The general result of the transformation in both cases of Secs. III A 1 and III A 2 is the following: As soon as the easy axis of uniaxial anisotropy coincides with one of the biaxial easy axes, becoming effective if $K_u = 0$, the generic terms in Eq. (2) are of opposite sign and $b < 0$. This means that in all such cases the same behavior can be expected on applying fields. In particular, the system is represented by the phase diagram given in Fig. 2 with the negative ordinate, corresponding to a field, applied along the easy axis. The positive ordinate represents a field direction along the hard axis. Hence, the field-driven spin reorientation in such systems will proceed via crossing the region of coexisting phases.

B. Magnetic easy axes deviating from in-plane axes of cubic symmetry

The second class of generic behavior of systems with an in-plane orientation of **M** occurs if the uniaxial easy axis deviates from the easy directions of the higher-order fourfold anisotropy. This situation is described by Eq. (3) if $K_4 < 0$ or by Eq. (6) if $K_4 > 0$, a situation that can be expected for Ni/Fe bilayer films on vicinal Ag(001) (Refs. 1,2) and for certain thicknesses of Co/Cu(110).[21,22] From the above transformations, *it follows that now b is positive*, while the sign of a depends on the relative strength of K_u and K_4. With b positive, the spin reorientation will proceed via a phase of canted magnetization with the magnetization tilted with respect to the principal symmetry axes. As a corollary, in this second generic case there is no new mathematics involved, but as a mere consequence of the treatment it follows that $b > 0$ and the physics of reorientation switches to the continuous canting nonhysteretic scenario.[9]

IV. COMPARISON WITH EXPERIMENTAL FINDINGS

A. General conclusions

The transformations given in the last paragraph demonstrate that films grown on vicinal low-index surfaces, exhibiting in-plane anisotropy, can be understood in the framework of phase diagrams such as that in Fig. 2. In order to put the phase diagram in a one-to-one correspondence with the particular systems in greater detail, we have to determine $r = a/b$ (the ratio of first-order to second-order anisotropies) which reads

$$r = -1 - \frac{|K_u|}{|K_4|} \leqslant -1 \tag{9}$$

for both situations with $b < 0$. In Eq. (9), we have evoked the relevant sign conventions from the above discussion. As an immediate consequence, ferromagnetic films grown on vicinal surfaces are mapped onto a portion of the diagram only. This is the portion of the $\overline{H}/r$ plane bounded by the line $r = -1$ and encompassing the side of arbitrary large negative r's.[23] When external fields are applied along the in-plane hard axis, this is represented by a vertical line in the second quadrant (see Fig. 2). The crossing of the regime of coexisting phases, and hence the hysteresis parts in the magnetization curves, are possible only within a certain r-range,[9] i.e., within the interval $-6 < r < -2$. Approaching the point $r = -6$ means that the two discontinuities in the field-dependent magnetization (X_L and X_N in Fig. 2) coalesce and finally disappear, while the transition from canted to conforming magnetization orientation becomes continuous. In the vicinity of $r \leqslant -2$, the lower-field discontinuity X_L shifts towards zero field. For $-2 \leqslant r \leqslant -1$, conventional hystereses arise even in the hard-axis experiment.

From these considerations one can determine the bounds for the anisotropy constants within which hard-axis loops will exhibit hysteresis effects at nonzero fields (offset hysteresis loops). Using Eq. (9), one obtains the bounds $|K_4| < |K_u| < 5|K_4|$. Vice versa, as soon as such offset loops ap-

pear in the hard-axis experiment, the anisotropies are bound by the above inequalities. This immediately brings us to the conclusion that *both anisotropy constants are of the same order of magnitude*. Hence, the assumption often made that one of the anisotropy constants is negligibly small[5–8] is plainly inconsistent with the magnetization loops observed.

The exact loci of the instabilities in the magnetization curves are given in Ref. 9 as

$$\bar{H}_L = -(2+r)/4, \tag{10}$$

$$\bar{H}_N = (-r)^{3/2}/216 \tag{11}$$

for the discontinuous transitions at X_L and X_N, respectively (see Fig. 2). With the definition of r and accounting for the normalization of $\bar{H}$, one obtains for the lower switching field at X_L

$$H_L = -2(|K_4| - |K_u|)/M \tag{12}$$

and for the higher switching field at X_N

$$H_N = \sqrt{\frac{8}{27|K_4|}} \cdot (|K_4| + |K_u|)^{3/2}/M. \tag{13}$$

Both discontinuous-transition fields are functions of K_4 and K_u, none of which can be neglected since they are close in magnitude, in contradiction with assumptions in recent papers.[5–8] Another characteristic field can also be given from the generalized theory.[9] This is the field H_{equ} where the two mimima for canted and conforming magnetization orientations are equal. From Ref. 9 it can be derived that

$$H_{\mathrm{equ}} = \frac{1}{\sqrt{2}} \cdot H_N. \tag{14}$$

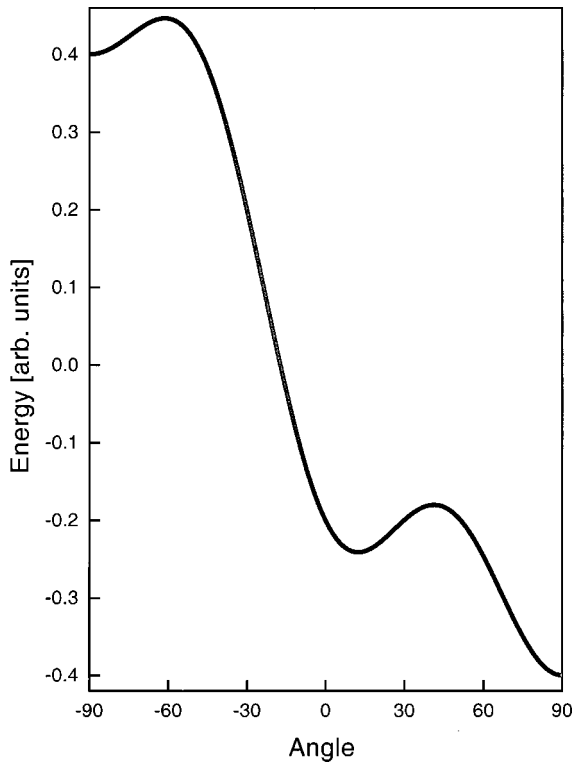

FIG. 4. Plot of angle-dependent energy [Eq. (2)] for $K_u = K_4/4$ and $H = 57$ Oe. The anisotropy values have been obtained from Fig. 1 under the assumption that the switching field $H_S = H_u = 60$ Oe. The magnetic field is acting along the $+90°$ direction. In the experiment the magnetization switches back at 57 Oe from a direction parallel to H into a direction close to $0°$. An absolute minimum appears in the field direction that will cause the magnetization to stay along that direction, in contradiction to the results presented in Fig. 1.

B. Analysis of an archetypal case [Co/Cu(1117]

Now we analyze Fig. 1 as a typical result representing the hysteresis of hard-axis experiments for in-plane magnetized films.[5–8,24–26] In particular, it will be demonstrated how anisotropy fields can be deduced by careful analysis. In carrying it out, we adopt a step-by-step interpretational procedure. At each stage, we formulate the assumptions which are most often used, usually implicitly. We then show that discrepancies arise which require improvements of the physical model of reorientation. Using only indisputable predictions of the general theory given in the preceding, we are able to definitely rule out misinterpretations of experimental data. Thus, at the final stage of the step-by-step argumentation one is left with a quantitatively consistent interpretation of offset hystereses. The procedure also helps delineate the limitations of the coherent-rotation model.

1. First interpretational ansatz

At first, we will apply the ansatz that is commonly used in literature to analyze this kind of hard-axis hysteresis.[8] The median of the two fields of discontinuous magnetization H_S is assumed to be directly related to the uniaxial anisotropy. For the data plotted in Fig. 1, one arrives at $H_s = H_u \approx 60$ Oe and to the anisotropy field $H_K = 300$ Oe (see Sec. I). With Eq. (1) we can calculate the fourfold contribution $H_4 = 240$ Oe. The analysis reveals that the fourfold anisotropy is roughly four times larger than the uniaxial contribution. A plot of the appropriate angle-dependent energy in a field $H = 57$ Oe applied along the in-plane hard axis clearly reveals that the absolute minimum is still in the field direction (Fig. 4). Since the local minimum which is closer to the easy axis is higher, the system will remain in the field direction. A switching back will not occur in disagreement with the experiment (Fig. 1). Evidently, such data analysis gives a wrong set of anisotropy fields that are not appropriate to describe the energy of the film correctly.

Sticking to the small-angle assumption as a good approximation for the torques acting on the magnetic moments, we have to conclude that the assumption made in connection with the switching field $H_S = H_u$ is wrong. It is worthwhile mentioning that the same contradiction is found when analyzing the data given in literature.[5,8]

2. Literal implementation of the coherent-rotation model

Now the analysis will be performed within the framework of the model based on the ansatz of spin reorientation utilizing the formulas given above. In a straightforward application, the first step is to attempt a one-to-one correspondence of the proposed theoretical and the measured hysteresis. In comparison with the plot in Fig. 2 (see the inset), we have to

assign the fields of discontinuous magnetization changes, i.e., at 57 and 61 Oe (see Sec. I), to the fields H_L/H_N, respectively. Applying the formulas derived in Sec. III and utilizing the zero field slope ($H_K=300$ Oe), we obtain after some mathematical manipulations that $H_N^2 > \frac{1}{7}\cdot H_K^2$ (see Appendix A). Inserting the numbers ($H_L/H_N=57$ and 61 Oe) into the formula, it turns out that the data do not satisfy the given inequality. Hence, we must deduce that the theory of Sec. III does not describe properly the set of experimental data when the zero-field slope is used. This is because some implicit assumptions, made when identifying the switching fields as H_L and H_N, are not fulfilled. The strongest prerequisite is that the discontinuous change of magnetization proceeds via coherent rotation. If the magnetization changes via nucleation of domains and domain wall propagation, the switching field will be strongly determined by microscopic properties and deviate from the values predicted by the model.[24,25] As the model is based on very general considerations about the film symmetry, it seems reasonable to stick to those physical features, as, e.g., the free-energy landscape, which are valid beyond the computational detail.

3. Inconsistent nucleation scenario

In the case of the nucleation-propagation mode we have to postulate that a second local minimum of the angle-dependent energy along the field direction is created upon applying the field. One possible ansatz is to assume that the switching happens when the minima along the field direction and the easy axis (in zero field) are equivalent (equally deep). This idea was recently put forward for the interpretation of hard-axis loops for the uniaxial in-plane system Fe/W(011).[26] As two minima are only found within the anisotropy range with coexisting phases, we can apply the general considerations of Sec. III once again. Equation (14) gives the relation between the hard-axis field and anisotropy in the case of equal minima. Applying that relation, assuming $H_{\mathrm{equ}}=60$ Oe and $H_K=300$ Oe, we obtain $H_u<H_4/10$ (see Appendix B). In Fig. 4, we have already plotted the case for $H_u<H_4/4$. In the case of even weaker uniaxial anisotropy the differences of the minima should be even stronger favoring the alignment of magnetization with the field direction. A switching back is even less probable than in the former case. Thus the experiment is not adequately described by the seemingly plausible assumption of switching at equivalent minima.

This example demonstrates that the exact solution derived from the theory of the spin reorientation in field helps perform different crosschecks to prove assumptions and/or models. Up to this point, we conclude that (i) the magnetization does not rotate coherently; (ii) assuming a switching via nucleation and propagation, it becomes obvious that the corresponding states between which the switching occurs are not those that have equal local minima.

4. The consistent interpretation

If we stick to the idea that a local minimum of the free energy must exist for both orientations of magnetization, we are fixed to the range of coexisting phases. A point is reached when the second local minimum appears first on increasing the field, i.e., when the field drives the film across the lower bound of the range of coexisting phases (Fig. 2). Following that idea, we can allocate the lowest field of discontinuous change of magnetization to H_L. Using the zero field slope, i.e., $H_K=300$ Oe, we find $H_u=178.5$ Oe, $H_4=121.5$ Oe, and $r=-2.47$, when applying Eq. (9). These numbers are reasonable and agree perfectly with all the conditions deduced from the general model. Plotting the angle dependent energy in a field of $H=57$ Oe a twofold symmetry is obtained (Fig. 5). At that particular field a local *maximum* still persists along the field direction (see inset a). As soon as the field is increased, a local minimum appears in the field direction (see inset b for $H=61$ Oe) *which can be populated in the magnetization switching via the nucleation-propagation mode*. Presumably, the nucleation is supported by inhomogeneous demagnetizing fields at the film edges and the system can overcome the remaining energy barrier.[26] Decreasing the field, the system will switch back as soon as the minimum is erased, i.e., at 57 Oe in the present case.

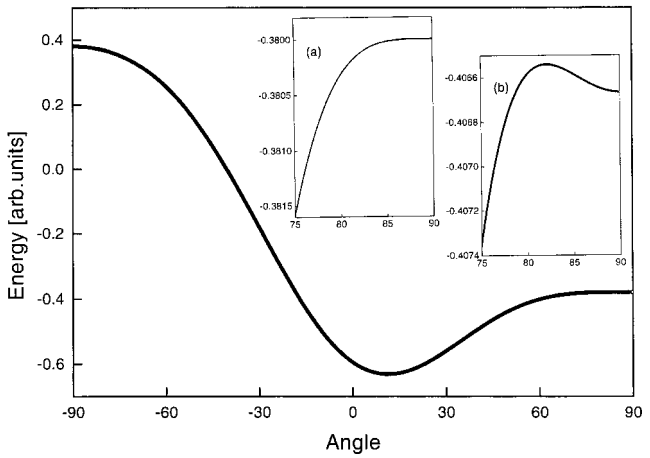

FIG. 5. Angle dependent energy with a field acting along the $+90$ direction. The field strength is 57 Oe while $H_u=178.5$ Oe and $H_4=121.5$ Oe. Note that the absolute minimum is not along the zero-field easy axis (0°). Inset (a) shows an enlarged section of the graph between 75° and 90°. The plot in (b) represents the same angle range when the field strength is slightly increased to 61 Oe. A minimum is found along the field direction in (b).

So far the analysis is in accordance with all possible checks derived from general considerations in the previous paragraphs. The theoretical treatment given in Ref. 9 allows a further quantitative check. The value of the magnetization in the different states can be calculated from the general solution of the theoretical treatment. The magnetization projection in the field direction is described by solution X_3 in the canted regime.[9] At H_L one obtains for the magnetization component along the ''hard axis'' $m_{HA}=0.20$, utilizing the anisotropy fields determined above from the hysteresis (see Appendix C). The experiment (Fig. 1) gives a component $m_{\mathrm{HA}}=0.21\pm0.01$ which is quite close to the theoretical value. This demonstrates that the state of magnetization at the lower discontinuity is nearly the same in general theory and experiment. The close agreement reveals that the ansatz is correct which assumes that the flop happens close to the low-field phase boundary of the range of coexisting phases.

C. The system Fe on curved Ag(001)

To demonstrate the applicability of the general treatment we finally perform the same analysis with a set of data from

the literature for a different system, i.e., Fe on curved Ag(001).[5] Taking the plot for $\alpha = 7.8°$ from Fig. 2 in Ref. 5, we obtain for the different fields $H_K = 941$ Oe and $H_L = 115.5$ Oe, respectively. This gives along the lines of the analysis in Sec. IV B 4 that $H_U = 528.25$ Oe, $H_4 = 412.75$ Oe, and $r = -2.28$, which again fulfil the conditions derived from the general theory. From the same plot in Fig. 2 of Ref. 5 we can also estimate the tilting of magnetization, i.e., the field-resolved magnetization component, at the lower flop field which is $m_{\mathrm{HA}} = 0.13 \pm 0.015$. With the theoretical solution X_3 for the magnetization component (see above), we get $m_{\mathrm{HA}} = 0.124$ in the case of $r = -2.28$.[27] The close agreement between calculated and measured values confirms that the two states involved in the flop transition are well described by the general theory. Vice versa, it demonstrates that the anisotropy values obtained by this analysis give the correct description of the angle dependent magnetic energy states. The analysis reveals that the hard-axis hysteresis achieved for Fe on curved Ag(001) (Ref. 5) can be understood and interpreted in the same way as those found for Co/Cu(1117).

V. CONCLUSIONS

A general classification for films with in-plane magnetization exhibiting uniaxial anisotropy is made. Based on the transformation onto the symmetry-adapted generalized mathematical structure, the influence of external fields applied along the hard axes is described. It is shown that for ultrathin films grown on vicinal surfaces with in-plane magnetization a field-driven spin reorientation via a state of coexisting phases appears. The coexistence of two phases in the field is responsible for the appearance of discontinuous magnetization jumps in hard-axis loops. It is demonstrated that hard-axis loops can be understood and analyzed in the framework of the model. Applying the model to Co/Cu(1 1 17) films as well as to Fe on curved Ag(001), the anisotropy constants involved are derived from the hard-axes curves. It is shown that for both film systems the magnetization reversal proceeds via domain nucleation and domain wall motion, and not via a coherent rotation.

APPENDIX A

From Eq. (12), we obtain

$$H_L = \frac{2}{M}(|K_u| - |K_4|) = H_u - H_4, \tag{A1}$$

and with Eq. (1) we can write

$$H_4 = \frac{1}{2}(H_K - H_L). \tag{A2}$$

From Eq. (13) we get

$$H_N = \sqrt{\frac{8}{27|K_4|}}\sqrt{\frac{M}{8}}\left\{\frac{2}{M}(|K_4| + |K_u|)\right\}^{3/2} = \sqrt{\frac{2}{27}}H_4^{-1/2}H_K^{3/2}; \tag{A3}$$

thus, one finally obtains

$$H_N^2 = \frac{4}{27}\frac{H_K^3}{H_K - H_L} > \frac{1}{7}H_K^2. \tag{A4}$$

APPENDIX B

Starting with Eq. (14) and following the above simplifications, we obtain

$$H_{\mathrm{equ}}^2 = \frac{1}{27}\frac{H_K^3}{H_4}. \tag{B1}$$

With the value for $H_{\mathrm{equ}} = H_K/5$ from the hysteresis (see text), we get

$$H_4 = \frac{25}{27}H_K, \tag{B2}$$

$$H_u = \frac{2}{27}H_K, \tag{B3}$$

respectively.

APPENDIX C

From the successful analysis of the data we can determine the general parameter p of the mathematical construct:[9]

$$p = r/2 = -1.235. \tag{C1}$$

For the ''linear'' boundary the equation $p + q + 1 = 0$ is valid[9] which yields

$$q = -1 - p = 0.235. \tag{C2}$$

The solution for the canted regime with r and b negative is X_3 which has the form[9]

$$X_3 = -2R\cos\left(\frac{\phi}{3} + \frac{4\pi}{3}\right) \tag{C3}$$

with

$$R = \mathrm{sgn}(q)\sqrt{\frac{|p|}{3}}, \tag{C4}$$

$$\phi = \arccos\left(\frac{q}{2R^3}\right). \tag{C5}$$

With the values for p and q we obtain $R = 0.642$ and $\phi = 1.102$ which gives for the component of the magnetization $X_3 = 0.196$.

*On leave from the Laboratory for Complex Phenomena in Condensed Systems, Institute of Solid State Physics, Bulgarian Academy of Sciences, Sofia.

[1] B. Heinrich, S. T. Purcell, J. R. Dutch, K. B. Urquart, J. F. Cochran, and A. S. Arrott, Phys. Rev. B **38**, 12 879 (1988).

[2] B. Heinrich and J. F. Cochran, Adv. Phys. **42**, 523 (1993).

[3] A. Berger, U. Linke, and H. P. Oepen, Phys. Rev. Lett. **68**, 839 (1992).

[4] J. Chen and J. Erskin, Phys. Rev. Lett. **68**, 1212 (1992).

[5] R. K. Kawakami, E. J. Escorcia-Aparicio, and Z. Q. Qiu, Phys. Rev. Lett. **77**, 2570 (1996).

[6] H. J. Choi, Z. Q. Qiu, J. Pearson, J. S. Jiang, Dongqi Li, and S.D. Bader, Phys. Rev. B **57**, R12 713 (1998).

[7] W. Weber, A. Bischof, R. Allenspach, C. Würsch, C. H. Back, and D. Pescia, Phys. Rev. Lett. **76**, 3424 (1996).

[8] W. Weber, C.H. Back, A. Bischof, C. Würsch, and R. Allenspach, Phys. Rev. Lett. **76**, 1940 (1996).

[9] Y. T. Millev, H. P. Oepen, and J. Kirschner, Phys. Rev. B **57**, 5837 (1998); **57**, 5848 (1998).

[10] W. Wulfhekel, S. Knappmann, and H. P. Oepen, J. Magn. Magn. Mater. **163**, 267 (1996) (Fig. 4).

[11] H. P. Oepen, C. M. Schneider, D. S. Chuang, C. A. Ballentine, and R. C. O'Handley, J. Appl. Phys. **73**, 6186 (1993).

[12] W. Wulfhekel, S. Knappmann, and H. P. Oepen, J. Appl. Phys. **79**, 988 (1996).

[13] Y. T. Millev and J. Kirschner, Phys. Rev. B **54**, 4137 (1996).

[14] S. Nieber and H. Kronmüller, Phys. Status Solidi B **165**, 503 (1991).

[15] A. I. Mitsek, N. P. Kolmakova, and D. I. Sirota, Fiz. Met. Metalloved. **38**, 35 (1974).

[16] C.-R. Chang and D. R. Fredkin, J. Appl. Phys. **63**, 3435 (1988).

[17] J. C. Oliveira de Jesus and W. Kleemann, J. Magn. Magn. Mater. **169**, 159 (1997).

[18] A. Aharoni, *Ferromagnetism* (Oxford University Press, Oxford, 1996).

[19] A. Hubert and R. Schäfer, *Magnetic Domains* (Springer, Berlin, 1998).

[20] The same result is obtained using the notation in Ref. 7 $a=K_u+K_1>0$ and $b=-K_1<0$ with positive K_u and K_1.

[21] J. Fassbender, C. Mathieu, B. Hillebrands, G. Güntherodt, R. Jungblut, and M. T. Johnson, J. Magn. Magn. Mater. **148**, 156 (1995).

[22] J. Fassbender, G. Güntherodt, C. Mathieu, B. Hillebrands, R. Jungblut, J. Kohlhepp, M. T. Johnson, D. J. Roberts, and G. A. Gehring, Phys. Rev. B **57**, 5870 (1998).

[23] In the treatment given here the restriction $r<-1$ will be observed, as an easy-axis flipping (in zero field) will not be considered.

[24] J. R. Childress, R. Kergoat, O. Durand, J.-M. George, P. Galtier, J. Miltat, and A. Schuhl, J. Magn. Magn. Mater. **130**, 13 (1994).

[25] R. P. Cowburn, S. J. Gray, J. Ferre, J. A. C. Bland, and J. Miltat, J. Appl. Phys. **78**, 7210 (1995).

[26] O. Fruchart, J.-P. Nozieres, and D. Givord, J. Magn. Magn. Mater. **165**, 508 (1997).

[27] With $r=-2.28$ we obtain $p=-1.14$, $q=0.14$, $R=0.616$, $\phi=1.267$ and finally $X_3=0.124$, following the sequence of calculations given in Appendix C.